Organic & Biomolecular Chemistry

Cite this: DOI: 10.1039/c2ob25351h

www.rsc.org/obc

PAPER

Regulation of NH-tautomerism in N-confused porphyrin by *N*-alkylation†

Motoki Toganoh,[a] Takaaki Yamamoto,[a] Takayoshi Hihara,[a] Hisanori Akimaru[a] and Hiroyuki Furuta*[a,b]

Received 19th February 2012, Accepted 3rd April 2012
DOI: 10.1039/c2ob25351h

A variety of internally *N*-alkylated N-confused porphyrins were prepared in a stepwise manner through the protection of the reactive peripheral nitrogen atom. NH-Tautomerism in N-confused porphyrins was found to be regulated by *N*-alkylation, which enabled us to obtain discrete information on two important NH-tautomers of an N-confused porphyrin.

Introduction

NH-Tautomerism is an important phenomenon in porphyrins and related compounds. In particular it plays a unique role in unsymmetrical porphyrinoids such as corrole,[1] N-confused porphyrins,[2] and N-fused porphyrins,[3] since the electronic structures as well as the photophysical properties change significantly through NH-tautomerization. Considering the potential applications of porphyrins and related compounds, it is important to address the regulation and better understanding of their properties. Usually NH-tautomers exist under equilibrium and the tautomeric ratio is dependent on solvents, additives, temperature, and so on. Thus, the study or comparison of each NH-tautomer under similar experimental conditions is usually difficult. One remedy for this problem is *N*-alkylation. Through *N*-alkylation, NH-tautomerization is intrinsically prevented and the porphyrin could be fixed as one type of tautomer.

An N-confused porphyrin (NCP) is a porphyrin isomer, which possesses an unsymmetrical structure unlike regular porphyrin.[4] Because of its unsymmetrical nature, there exist six NH-tautomers in NCP (Fig. 1). These tautomers can be categorized into two groups.[2,5] When the N-confused pyrrole ring takes an imino form, those tautomers are categorized as type-A. Type-A tautomers possess [18]annulenic circuits and show strong aromaticity. On the other hand, when the N-confused pyrrole ring takes an amino form, those tautomers are categorized as type-B. Type-B tautomers do not have [18]annulenic circuits and show moderate aromaticity. The equilibrium between type-A tautomers and type-B tautomers can be controlled by external stimuli and,

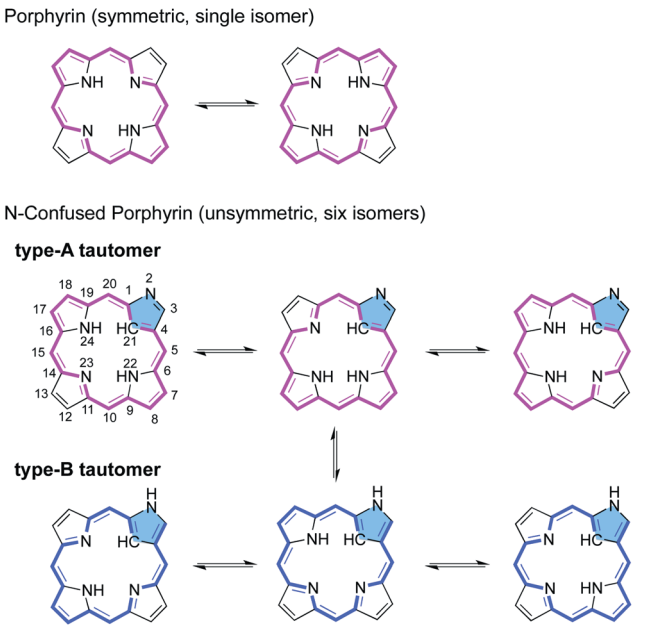

Fig. 1 NH-Tautomerism in porphyrins and N-confused porphyrins.

combined with the very different characters of type-A and type-B tautomers, further applications would be promising.[6] Nevertheless, the fundamental understanding of each NH-tautomer is still immature and an important subject to address.

This time, to fix the NH-tautomers of NCPs, *N*-alkylation reactions inside the macrocycle were examined (Fig. 2). Although *N*(23)-alkyl NCP was not obtained by direct alkylation, this missing isomer was synthesized by a [3 + 1] acid condensation reaction, separately. With a set of *N*-alkyl N-confused porphyrins in hand, the fundamental properties of each NH-tautomer were investigated experimentally as well as theoretically. In addition, the comparison of *N*(22)-alkyl NCP and *N*(24)-alkyl NCP gave insight into the unsymmetric nature of N-confused porphyrins.

[a]*Department of Chemistry and Biochemistry, Graduate School of Engineering, Kyushu University, 744 Motooka, Nishi-ku, Fukuoka 819-0395, Japan. E-mail: hfuruta@cstf.kyushu-u.ac.jp; Fax: +81 92-802-2865*
[b]*International Research Center for Molecular Systems, Kyushu University, 744 Moto-oka, Nishi-ku, Fukuoka 819-0395, Japan*
† Electronic supplementary information (ESI) available. CCDC 856308, 856309. For ESI and crystallographic data in CIF or other electronic format see DOI: 10.1039/c2ob25351h

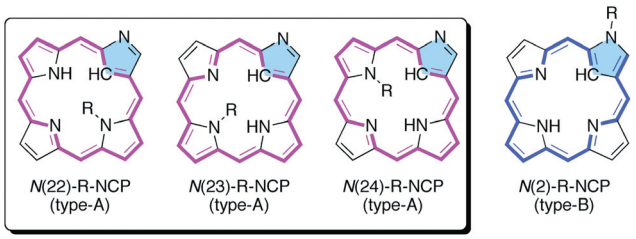

Fig. 2 Regulation of NH-tautomerism by *N*-alkylation in N-confused porphyrin.

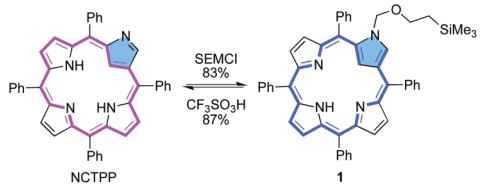

Scheme 1 Protection and deprotection of NCTPP.

Results and discussion

Synthesis of inner *N*-alkyl N-confused porphyrins

The first *N*-alkylation reaction of NCP was reported soon after its discovery.[7] The reaction of free-base NCP with an alkyl halide proceeded exclusively at the peripheral nitrogen atom or the *N*(2)-position to afford *N*(2)-alkyl NCP. This peripheral modification reaction is readily achieved and thus often utilized for peripheral modification of NCP.[8] Further alkylation of *N*(2)-alkylated NCP proceeded at the interior nitrogen atoms or the *N*(22)/*N*(24)-positions to give dialkylated NCP.[9]

To obtain inner *N*-alkylated NCP with an intact N-confused pyrrole ring, we relied on the protection of NCP. Thus, upon treatment of N-confused tetraphenylporphyrin (NCTPP) with an excess amount of 2-(trimethylsilyl)ethoxymethyl chloride (SEMCl)[10] at 27 °C for 1 d, *N*(2)-SEM-NCTPP (**1**) was obtained in 83% yield (Scheme 1).[11] Deprotection of the SEM group can be achieved with F^- or acid. For example, treatment of **1** with CF_3SO_3H gave NCTPP in 87% yield. The structure of **1** was confirmed by X-ray crystallographic analysis (Fig. 3).‡ The N-confused pyrrole ring (5 heavy atoms) is tilted relative to the rest mean porphyrin plane (19 heavy atoms) by 24.7°.

N-Alkyl-NCTPPs were prepared by alkylation of **1** and subsequent deprotection (Scheme 2). Upon treatment of **1** with excess MeI in CH_2Cl_2 in the presence of Et_3N, a crude mixture of **2** and **3** was obtained after passing though a pad of silica gel. Since separation of **2** and **3** by standard silica gel column chromatography was troublesome due to their high polarity, deprotection was achieved directly on the crude mixture with CH_3SO_3H

‡ *Crystallographic data* **1**: $C_{50}H_{44}N_4OSi$, M_W 744.98, triclinic, space group $P\bar{1}$ (No. 2), a = 10.344(4), b = 13.082(5), c = 14.935(6) Å, V = 1976.4(13) Å^3, Z = 2, T = 223 K, R = 0.0620 ($I > 2\sigma(I)$), R_W = 0.1653 (all data), GOF on F^2 = 0.854 (all data), CCDC reference number 856308. **4**·CH_2Cl_2: $C_{46}H_{34}Cl_2N_4$, M_W 713.67, triclinic, space group $P\bar{1}$ (No. 2), a = 10.881(4), b = 12.396(5), c = 14.261(6) Å, V = 1775.4(12) Å^3, Z = 2, T = 123 K, R = 0.0686 ($I > 2\sigma(I)$), R_W = 0.1872 (all data), GOF on F^2 = 01.060 (all data), CCDC reference number 856309.

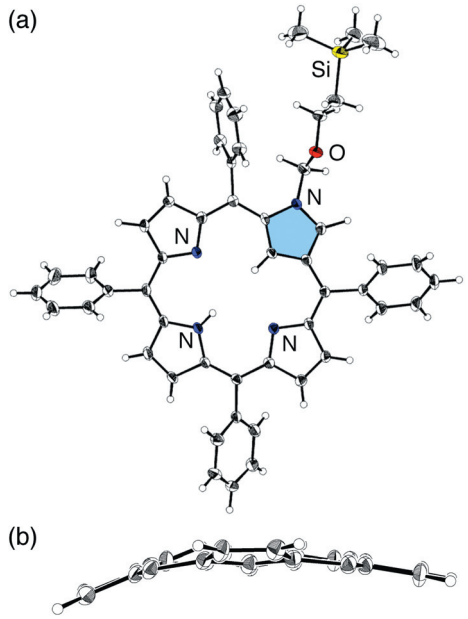

Fig. 3 X-Ray structure of **1**: (a) top view, (b) side view. The thermal ellipsoids are shown at the 30% probability level. The SEM group and *meso*-phenyl groups are omitted for clarity in (b).

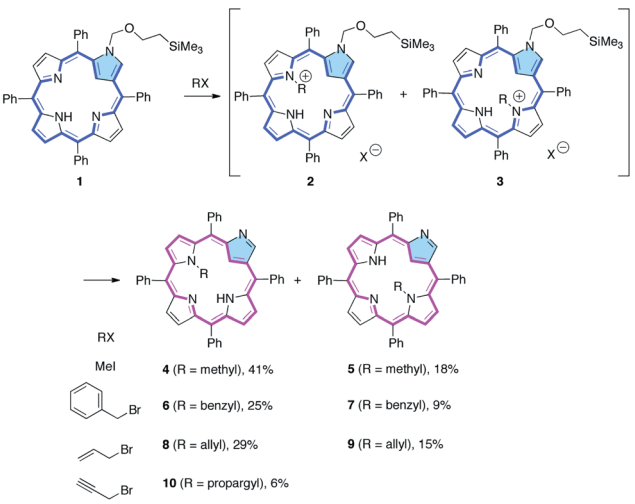

Scheme 2 Preparation of *N*(24)-alkyl-NCTPP and *N*(22)-alkyl-NCTPP.

to give *N*(24)-methyl-NCTPP (**4**) and *N*(22)-methyl-NCTPP (**5**) in 41% and 18% yield (2 steps), respectively. The ^{1}H NMR signals assignable to the NMe moiety inside the macrocycle appeared at δ −2.83 (**4**) and −3.24 ppm (**5**), respectively. In a similar fashion, a variety of inner *N*-alkyl-NCTPPs were synthesized. The reaction with benzyl bromide afforded *N*(24)-benzyl-NCTPP (**6**, 25% yield) and *N*(22)-benzyl-NCTPP (**7**, 9% yield), and the reaction with allyl bromide afforded *N*(24)-allyl-NCTPP (**8**, 29% yield) and *N*(22)-allyl-NCTPP (**9**, 15% yield). Meanwhile, the reaction with propargyl bromide only afforded *N*(24)-propargyl-NCTPP (**10**) in 6% yield. In these reactions, production of *N*(23)-alkyl-NCTPP was not observed so far.

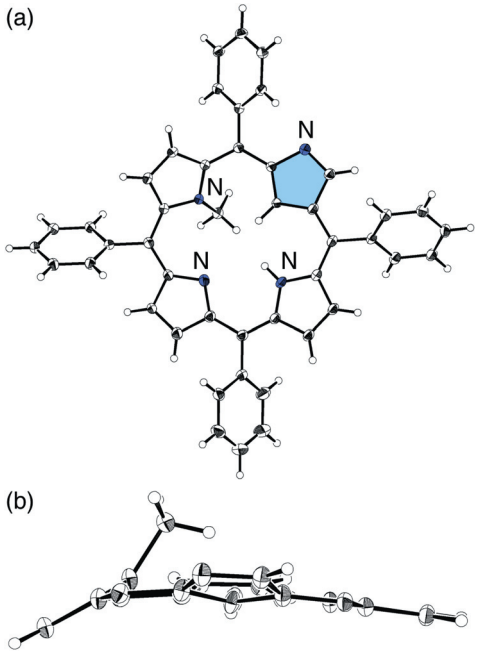

Fig. 4 X-Ray structure of **4**: (a) top view, (b) side view. The thermal ellipsoids are shown at the 30% probability level. The *meso*-phenyl groups are omitted for clarity in (b).

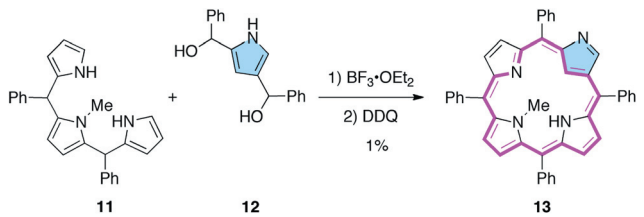

Scheme 3 Preparation of *N*(23)-methyl-NCTPP.

The structure of **4** was confirmed by X-ray crystallographic analysis, where the methyl group was installed to the *N*(24)-position (Fig. 4).‡ The *N*-methyl pyrrole ring (5 heavy atoms) is tilted relative to the rest mean porphyrin plane (19 heavy atoms) by 34.1°. The standard deviation from the mean plane of **4** is 1.429 Å, which is comparable to that of free-base NCTPP (1.426 Å). Thus, the planarity of the N-confused porphyrin skeleton is not lost significantly by installation of the inner *N*-alkyl group, which was further supported by a negligible substituent effect on the absorption spectra of inner *N*-alkylated NCTPPs.

Although *N*(23)-alkyl NCP was not obtained by alkylation of NCP derivatives, it could be synthesized by a [3 + 1] acid condensation reaction (Scheme 3). Thus, treatment of 16-methyl-5,10-diphenyltripyrrane (**11**)[12] and 2,4-di(phenylhydroxymethyl)pyrrole (**12**) with $BF_3{\cdot}OEt_2$ in CH_2Cl_2 followed by oxidation gave *N*(23)-methyl-NCTPP (**13**) albeit in low yield. While **13** decomposed readily during silica gel column separation, it could be isolated by standard alumina column separation. The ^{1}H NMR signal assignable to the NMe moiety appeared at δ −3.16 ppm, suggesting strong aromaticity of **13**.

Table 1 Comparison of type-A tautomer and type-B tautomer in NCTPP

	Type-A	Type-B	TPP
Relative energy (kcal mol^{-1})[a]	0.00	4.94	−12.29
$\Delta\delta_{CH-CH}$ (ppm)	14.00[b]	7.35[c]	—
NICS (ppm)[a]	−11.90	−6.03	−13.69
$HOMA_{18}$[a]	0.7863	0.7231	0.7625
HOMO (eV)[a]	−5.12	−4.82	−5.31
LUMO (eV)[a]	−2.78	−2.76	−2.57
HOMO–LUMO gap (eV)[a]	2.34	2.05	2.74
TDDFT (nm)[a]	656	714	579
Absorption (nm)	727[d]	682[e]	648[d]
Emission (nm)	748[d]	705[e]	653[d]
Quantum yield (%)[f]	2.3[d]	4.2[e]	4.8[d]
Stokes shift (cm^{-1})	386[d]	479[e]	118[d]

[a] Calculated at the B3LYP/6-311++G**//B3LYP/6-31G** level. [b] In $CDCl_3$. [c] In DMF-d_7. [d] In CH_2Cl_2. [e] In CH_2Cl_2 with excess $Bu_4N^+F^-$. [f] Absolute quantum yield.

Properties of type-A NCTPP and type-B NCTPP

Before discussing *N*-alkyl-NCTPP, the fundamental properties of type-A NCTPP and type-B NCTPP have been reviewed (Table 1).[13] The properties of tetraphenylporphyrin (TPP) are also shown for comparison. NCTPP takes the type-A form in CH_2Cl_2 while it takes the type-B form in DMF or in CH_2Cl_2 with excess $Bu_4N^+F^-$.[14] To obtain an experimental measure of aromaticity, the difference between the most shielded CH signal and the least shielded CH signals ($\Delta\delta_{CH-CH}$) is given. In the aromatic porphyrins, the most shielded signal is derived from a peripheral proton and the least shielded signal is derived from an interior proton. Thus a larger $\Delta\delta_{CH-CH}$ value indicates stronger aromaticity. The $\Delta\delta_{CH-CH}$ value of the type-A tautomer (14.00 ppm) indicates strong aromatic character and that of the type-B tautomer (7.35 ppm) indicates moderate aromatic character. The nucleus independent chemical shift (NICS)[15] values as well as the harmonic oscillator model of aromaticity for an [18] annulenic circuit ($HOMA_{18}$)[16] indices for type-A tautomers (NICS: −11.90 ppm, $HOMA_{18}$: 0.7863) and type-B tautomers (NICS: −6.03 ppm, $HOMA_{18}$: 0.7231) are in good agreement with experimental observation. Accordingly the type-B tautomer (2.05 eV) has a considerably narrower HOMO–LUMO band gap than the type-A tautomer (2.34 eV). Time-dependent density functional theory (TDDFT) calculations are consistent with the HOMO–LUMO gaps; the type-B tautomer (714 nm) exhibits a longer wavelength than the type-A tautomer (656 nm). However, the experimental absorption wavelength of the type-B tautomer (682 nm) was shorter than that of the type-A tautomer (727 nm) albeit under different measurement conditions. The mismatch between experimental and theoretical absorption wavelengths will be discussed later. The experimental emission wavelengths (748 nm for the type-A tautomer and 705 nm for the type-B tautomer) were in good agreement with the experimental absorption wavelengths. Type-B NCTPP (4.2%) showed a higher absolute emission quantum yield than type-A NCTPP (2.3%). The Stokes shifts of the type-A tautomer (386 cm^{-1}) and the type-B tautomer (479 cm^{-1}) are significantly larger than that of TPP (118 cm^{-1}). This could be due to the more flexible skeleton of NCTPP compared to that of TPP. The smaller HOMA index of

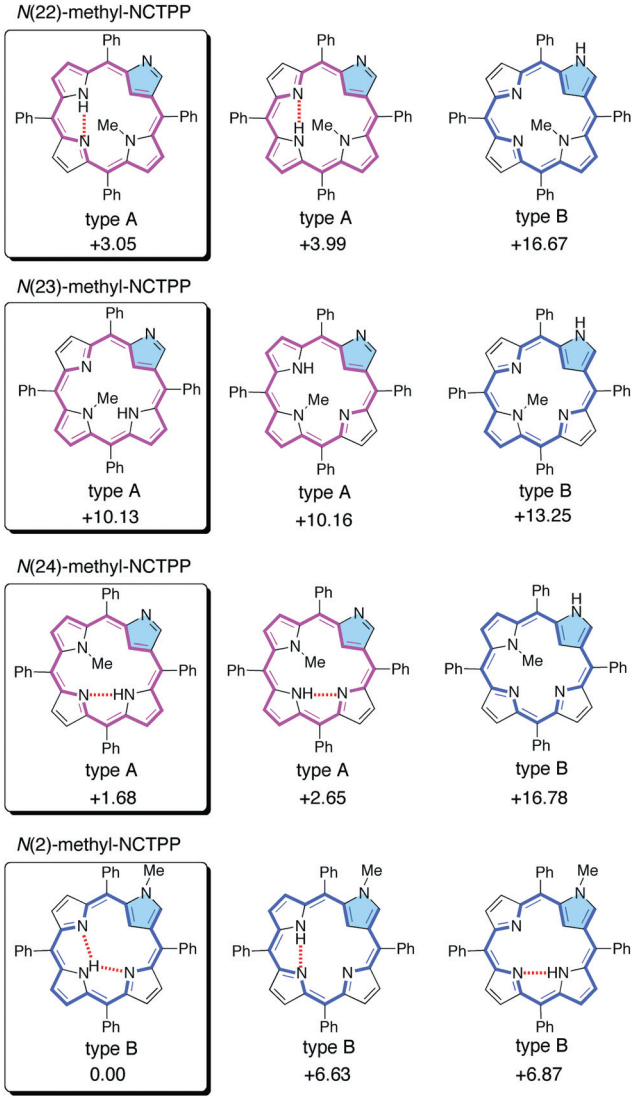

Fig. 5 NH-Tautomers of *N*-methyl NCTPPs. The numbers indicate relative energies (kcal mol^{-1}) at the B3LYP/6-31G** level calculation.

TPP (0.7625) than that of type-A NCTPP (0.7863) in spite of its highly negative NICS value (−13.69 ppm) might also indicate a more rigid or strained skeleton of TPP.

NH-Tautomerism of *N*-methyl-NCTPPs

The possible isomers and NH-tautomers for *N*-methyl-NCTPP are listed in Fig. 5 together with their relative thermodynamic stability. Usually, the relative stability of porphyrinoids is highly dependent on the intramolecular hydrogen bonding.[5] In the case of *N*(22)-methyl and *N*(24)-methyl NCTPP, we can describe two type-A tautomers and one type-B tautomer. Intramolecular hydrogen bonding is completely lost in the type-B tautomers, while the type-A tautomers do have intramolecular hydrogen bonding. Thus, the type-B tautomers are expected to be less stable. A DFT study showed that the type-B tautomers were less stable than the type-A tautomers by 13–15 kcal mol^{-1}. The large energy difference between type-A tautomers and type-B tautomers indicates that *N*(22)-methyl-NCTPP and *N*(24)-methyl-NCTPP exclusively take the type-A form under common experimental conditions. The ^{1}H NMR analysis of *N*(22)-methyl-NCTPP and *N*(24)-methyl-NCTPP showed that they formed type-A tautomers not only in $CDCl_3$ but also in DMF-d_7. Of course an equilibrium between the two type-A tautomers would exist in both cases. In the case of *N*(2)-methyl-NCTPP, only type-B tautomers are possible. Among the three NH-tautomers of *N*(2)-methyl-NCTPP in Fig. 5, the left-hand one is the most stable due to favorable intramolecular hydrogen bonding. Accordingly, we can measure the properties of type-A tautomers in polar solvents (or type-B tautomers in less-polar solvents) unlike intact NCTPP. Although type-A NCTPP was thermodynamically more stable than type-B NCTPP, *N*(24)-methyl-NCTPP (type-A) is less stable than *N*(2)-methyl-NCTPP (type-B) by 1.68 kcal mol^{-1}. This can be explained by the loss of intramolecular hydrogen bonding inside the core and steric repulsion imposed by the interior methyl group in *N*(24)-methyl-NCTPP. In *N*(23)-methyl-NCTPP, no intramolecular hydrogen bonding is expected in any NH-tautomers and also the energy differences among the NH-tautomers are relatively small. Nevertheless the type-A tautomers are more stable than the type-B tautomer by *ca.* 3 kcal mol^{-1}, which is consistent with the ^{1}H NMR observation. Only the type-A tautomers are observed not only in $CDCl_3$ but also in DMF-d_7. Besides, the two type-A NH-tautomers are observed independently in CD_2Cl_2 at −80 °C in a ratio of 85 : 15. This would suggest slow or indirect proton migration in *N*(23)-methyl-NCTPP. Both type-A and type-B *N*(23)-methyl-NCTPPs are less stable than the other *N*-methyl-NCTPPs due to loss of intramolecular hydrogen bonding, which would account for the absence of *N*(23)-alkyl-NCTPP in the direct inner-alkylation reactions of NCTPP.

Table 2 Properties of *N*-methyl-NCTPPs

	N(22)-methyl-NCTPP	*N*(23)-methyl-NCTPP	*N*(24)-methyl-NCTPP	*N*(2)-methyl-NCTPP
Tautomer type	A	A	A	B
Relative energy (kcal mol^{-1})[a]	3.78	10.54	2.57	0.00
$\Delta\delta_{CH-CH}$ (ppm)[b]	13.65	12.39	12.85	6.73
NICS (ppm)[a]	−11.40	−11.67	−10.91	−5.63
$HOMA_{18}$[a]	0.7905	0.7830	0.7751	0.7159
HOMO (eV)[a]	−4.99	−4.77	−4.99	−4.76
LUMO (eV)[a]	−2.75	−2.42	−2.73	−2.76
HOMO–LUMO gap (eV)[a]	2.24	2.35	2.26	2.00
TDDFT (nm)[a]	690	666	680	726
Absorption (nm)[c]	766	764	753	713
Emission (nm)[c]	786	836	780	752
Quantum yield (%)[c,d]	1.1	<0.1	1.5	2.5
Stokes shift (cm^{-1})[c]	332	1127	459	727

[a] Calculated at the B3LYP/6-311+G**//B3LYP/6-31G** level. [b] In $CDCl_3$. [c] In CH_2Cl_2. [d] Absolute quantum yield.

Properties of *N*-methyl-NCTPPs

The properties of *N*(22)-methyl-, *N*(23)-methyl-, *N*(24)-methyl-, and *N*(2)-methyl-NCTPPs are summarized in Table 2. The

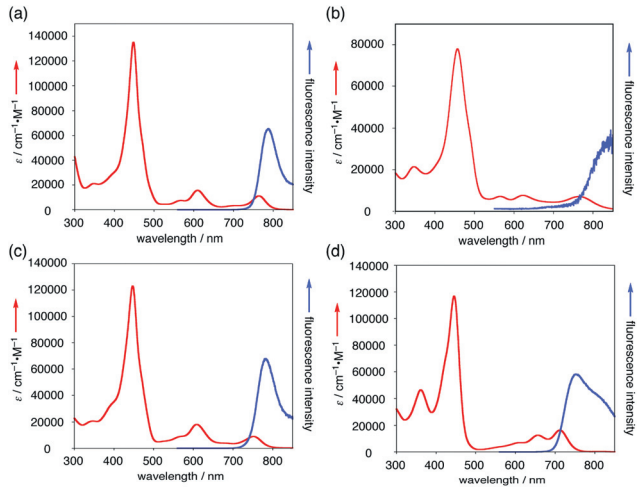

Fig. 6 Absorption and emission spectra of (a) *N*(22)-, (b) *N*(23)-, (c) *N*(24)-, (d) *N*(2)-methyl-NCTPP in CH_2Cl_2.

absorption and emission spectra in CH_2Cl_2 are shown in Fig. 6. As discussed above, *N*(22)-methyl-NCTPP and *N*(24)-methyl-NCTPP take the type-A form and *N*(2)-methyl-NCTPP takes the type-B form regardless of solvent polarity. Accordingly, the fundamental properties of *N*(22)-methyl-NCTPP and *N*(24)-methyl-NCTPP resemble those of type-A NCTPP, and the fundamental properties of *N*(2)-methyl-NCTPP resemble those of type-B NCTPP. The properties of *N*(23)-methyl-NCTPP are similar to those of type-A NCTPP except for some photophysical properties such as small solvent dependency and lower emission efficiency.

Comparison of *N*(24)-methyl-NCTPP and *N*(2)-methyl-NCTPP

The $\Delta\delta_{CH-CH}$ values suggests strong aromaticity of *N*(24)-methyl-NCTPP (12.85 ppm) and moderate aromaticity of *N*(2)-methyl-NCTPP (6.73 ppm). The NICS values of *N*(24)-methyl-NCTPP (−10.91 ppm) and *N*(2)-methyl-NCTPP (−5.63 ppm) are comparable to the $\Delta\delta_{CH-CH}$ values. Accordingly *N*(24)-methyl-NCTPP (0.7751) shows a larger HOMA index than *N*(2)-methyl-NCTPP (0.7159).

In TDDFT calculations, a longer absorption wavelength was obtained for *N*(2)-methyl-NCTPP (726 nm) than for *N*(24)-methyl-NCTPP (680 nm), which is consistent with the narrower HOMO–LUMO band gaps of the former (2.00 eV) than the latter (2.26 eV). Similarly to the case of intact NCTPP the theoretical wavelength does not match with the experimental wavelength (*N*(2)-methyl-NCTPP: 713 nm, *N*(24)-methyl-NCTPP: 753 nm), whereas the emission wavelengths of *N*(2)-methyl-NCTPP (752 nm) and *N*(24)-methyl-NCTPP (780 nm) still conform to the observed absorption wavelengths. The Stokes shift of *N*(2)-methyl-NCTPP (727 cm^{-1}) is larger than that of *N*(24)-methyl-NCTPP (459 cm^{-1}). It implies a higher skeletal flexibility of type-B tautomers than type-A tautomers, which is suggested by the previous theoretical study.[5] The emission quantum yields of *N*(2)-methyl-NCTPP (2.5%) and *N*(24)-methyl-NCTPP (1.5%) were smaller than those of type-B and type-A intact NCTPPs, respectively.

Comparison of *N*(24)-methyl-NCTPP and *N*(22)-methyl-NCTPP

Similar but slightly different properties between *N*(24)-methyl-NCTPP and *N*(22)-methyl-NCTPP would reflect the unsymmetrical nature of NCTPP. *N*(24)-Methyl-NCTPP is thermodynamically more stable than *N*(22)-methyl-NCTPP by 1.21 kcal mol^{-1}, which is consistent with the preferential production of *N*(24)-methyl-NCTPP over *N*(22)-methyl-NCTPP (69 : 31). In spite of its lower stability, *N*(22)-methyl-NCTPP shows stronger aromaticity than *N*(24)-methyl-NCTPP. For example, the $\Delta\delta_{CH-CH}$ value for *N*(22)-methyl-NCTPP (13.65 ppm) is larger than that for *N*(24)-methyl-NCTPP (12.85 ppm). The NICS values and HOMA indices are consistent with the $\Delta\delta_{CH-CH}$ values. Therefore, the higher stability of *N*(24)-methyl-NCTPP could be explained not by electronic factors but by steric factors. Namely, *N*(24)-methyl-NCTPP would have a slightly more flexible skeleton than *N*(22)-methyl-NCTPP, which could reduce the steric repulsion induced by the interior methyl group. In fact, the Stokes shift for *N*(24)-methyl-NCTPP (459 cm^{-1}) is considerably larger than that for *N*(22)-methyl-NCTPP (332 cm^{-1}) in spite of the close resemblance of their structures.

Comparison of *N*(24)-methyl-NCTPP and *N*(23)-methyl-NCTPP

Finally, the properties of *N*(23)-methyl-NCTPP are compared with *N*(24)-methyl-NCTPP. In spite of its lower stability, *N*(23)-methyl-NCTPP shows strong aromatic character comparable to *N*(24)-methyl-NCTPP. For example, the $\Delta\delta_{CH-CH}$ value of *N*(23)-methyl-NCTPP (12.39 ppm) is almost same as that of *N*(24)-methyl-NCTPP (12.85 ppm). Possibly due to the absence of intramolecular hydrogen bonding in *N*(23)-methyl-NCTPP, it has a more flexible skeleton than *N*(24)-methyl-NCTPP. In fact, the Stokes shift for *N*(23)-methyl-NCTPP (1127 cm^{-1}) is considerably larger than that for *N*(24)-methyl-NCTPP (459 cm^{-1}) and the emission quantum yield of *N*(23)-methyl-NCTPP (<0.1%) is much lower than that of *N*(24)-methyl-NCTPP. In TDDFT calculations, a longer absorption wavelength was obtained for *N*(24)-methyl-NCTPP (680 nm) compared to *N*(23)-methyl-NCTPP (666 nm), which is consistent with the narrower HOMO–LUMO band gap of the former (2.26 eV) than the latter (2.35 eV).

Solvent effect

The absence of NH-tautomerism in *N*-alkyl-NCTPPs enables us to measure the solvent effect on the photophysical properties for type-A and type-B tautomers, which is difficult to obtain for intact NCTPP. The absorption spectra of *N*(22)-methyl-, *N*(23)-methyl-, *N*(24)-methyl-, and *N*(2)-methyl-NCTPPs in a variety of solvents are shown in Fig. 7 together with the theoretical oscillator strengths. The absorption wavelengths are listed in Table 3. In almost all cases, the absorption wavelengths were almost completely insensitive to the solvent. Thus, photoabsorption in the Soret-band region as well as the Q-band region would correspond to a simple π–π* transition similarly to regular porphyrin. The contribution of intramolecular electron transfer should be negligible in any case. The theoretical oscillator strengths roughly fit with the experimental data, although some gaps are recognized in the Q-band region.[17] While no direct

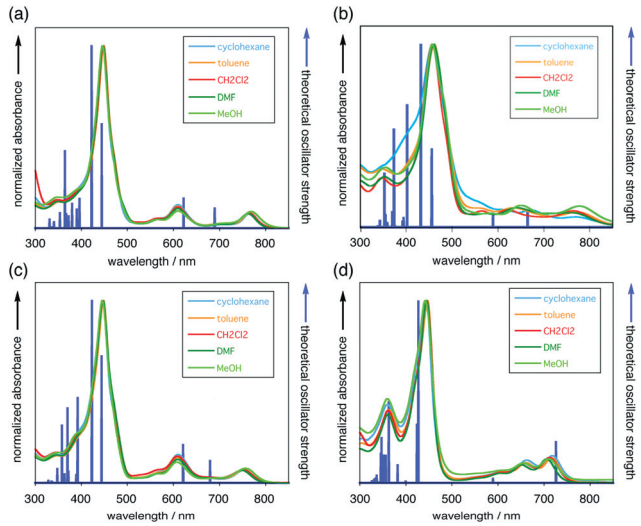

Fig. 7 Absorption spectra in a variety of solvents and theoretical oscillator strengths of (a) *N*(22)-, (b) *N*(23)-, (c) *N*(24)-, (d) *N*(2)-methyl-NCTPP.

evidence has been obtained yet, this mismatch would be due to vibrational levels, since a large splitting of the Q-band region at *ca.* 150 nm was recognized in *N*(22)-, *N*(23)-, and *N*(24)-methyl-NCTPPs. The small solvent dependency observed for *N*(23)-methyl-NCTPP might be explained by the high flexibility of its molecular skeleton.

Conclusions

An *N*-alkylation reaction inside the NCP core was developed and the properties of *N*-methyl-NCTPPs were investigated. Through *N*-alkylation, NH-tautomerism of NCPs can be regulated, which enabled us to obtain a deep insight into the difference between type-A and type-B tautomers of NCPs. The type-A tautomer had stronger aromaticity, narrower HOMO–LUMO gaps, and longer wavelength absorption than the type-B tautomer.

Unlike regular porphyrins, NCPs have a flexible skeleton and thus interior functionalization of NCPs often led to fascinating structures with unique properties such as N-fused porphyrins,[18] doubly N-fused porphyrins,[19] N-heterocyclic carbenes embedded in NCP,[20] etheno-bridged NCP,[21] imino-fused NCP,[22] and so on.[23] The versatile interior alkylation method developed here should lead to more interesting molecules in the near future.

Experimental

General

All the reactions were performed in oven-dried reaction vessels under Ar or N_2. Commercially available solvents and reagents were used without further purification unless otherwise mentioned. CH_2Cl_2 was dried by passing through a pad of alumina. Dry THF (stabilizer free) was purchased from KANTO and used as received. Thin-layer chromatography (TLC) was carried out on aluminum sheets coated with silica gel 60 F_{254} and aluminium oxide 60 F_{254}, neutral (MERCK). Preparative separation was performed by silica gel flash column chromatography (KANTO Silica Gel 60 N, spherical, neutral, 40–50 μm) or silica gel gravity column chromatography (KANTO Silica Gel 60 N, spherical, neutral, 63–210 μm). ^{1}H NMR spectra were recorded in $CDCl_3$ solution on a JNM-AL SERIES FT-NMR spectrometer (JEOL) at 300 MHz, and chemical shifts were reported relative to a residual proton of a deuterated solvent, $CHCl_3$ (δ = 7.26) in ppm. ^{13}C NMR spectra were recorded in $CDCl_3$ solution on the same instrument at 75 MHz, and chemical shifts were reported relative to $CDCl_3$ (δ = 77.00) in ppm. UV/vis/near-IR absorption spectra were recorded on a UV-3150PC spectrometer (Shimadzu) with a photomultiplier tube detector (190–750 nm) and a PbS detector (750–3200 nm). Emission spectra were recorded on an APEX Fluorolog-3-NIR spectrometer (HORIBA) with a photomultiplier tube detector (R928P: 240–850 nm). Fluorescence quantum yields were measured with a C9920-02 (Hamamatsu Photonics) absolute photoluminescence quantum yield measurement system with a data interval of 0.8 nm. All the quantum yield measurements were achieved three times and the averaged values are reported. Mass spectra were recorded on an autoflex MALDI–TOF MS spectrometer (Bruker Daltonics). High resolution mass spectra were measured with a JMS-T100CS (ESI mode, JEOL).

Preparation of *N*(24)-methyl-NCTPP (4) and *N*(22)-methyl-NCTPP (5) (typical procedure). Iodomethane (1.5 mL) was added to a solution of **1** (300 mg) in CH_2Cl_2 (5 mL) and the mixture was stirred at 23 °C. After 10 min, Et_3N (80 μL) was added and the resulting mixture was stirred for 24 h. The residue was evaporated and purified with silica gel column chromatography with CH_2Cl_2–MeOH = 99 : 1–95 : 5 (v/v). The brown band was collected and evaporated. To a solution of this residue in CH_2Cl_2 (50 mL), methanesulfonic acid (500 μL) was added and stirred for 4 h at 23 °C. After neutralization with Et_3N, the reaction mixture was evaporated to dryness. The residue was subjected to silica gel column chromatography with CH_2Cl_2–MeOH = 99 : 1–98 : 2 (v/v). The first and second green bands were collected respectively and evaporated to give **5** (46 mg, 18% yield, green solid) and **4** (104 mg, 41%, green solid), respectively.

4: ^{1}H NMR ($CDCl_3$, 300 MHz) δ −4.17 (s, 1H), −2.83 (s, 3H), −0.68 (br s, 1H), 7.11 (d, J = 4.6 Hz, 1H), 7.62 (d, J = 4.6 Hz, 1H), 7.72–7.90 (m, 13H), 8.05–8.06 (m, 1H), 8.16–8.22 (m, 4H), 8.28 (d, J = 4.8 Hz, 1H), 8.38 (d, J = 4.8 Hz, 1H), 8.44 (d, J = 4.8 Hz, 1H), 8.58 (d, J = 7.5 Hz, 2H), 8.67 (s, 1H), 8.68 (d, J = 4.8 Hz, 1H); ^{13}C NMR ($CDCl_3$, 300 MHz) δ 31.64, 107.15, 115.82, 119.44, 122.81, 124.50, 127.14, 127.22, 127.25, 127.52, 127.91, 127.94, 128.06, 128.82, 130.26, 131.24, 131.39, 133.64, 134.14, 134.34, 135.14, 136.83, 138.69, 138.78, 140.29, 140.53, 141.10, 142.90, 144.86, 149.00, 149.02, 150.90, 151.77, 152.45, 156.57, 159.02; MS (MALDI, positive) m/z = 629.1 (MH^+); HRMS (ESI^+): m/z: found: 629.26680, calcd for $C_{45}H_{33}N_4O_3$ (MH^+): 629.27052; UV-vis (CH_2Cl_2, λ_{max}/nm, (log ε) 448 (5.09), 609 (4.24), 753 (3.97); R_f 0.16 (CH_2Cl_2–MeOH 97 : 3).

5: ^{1}H NMR ($CDCl_3$, 300 MHz) δ −4.79 (s, 1H), −3.24 (s, 3H), −1.09 (br s, 1H), 7.28 (d, J = 4.8 Hz, 1H), 7.72–7.83 (m, 11H), 7.91 (t, J = 7.4 Hz, 2H), 8.06–8.09 (m, 1H), 8.25 (d, J = 7.4 Hz, 4H), 8.38–8.49 (m, 6H), 8.70 (d, J = 4.8 Hz, 1H), 8.86 (s, 1H); ^{13}C NMR ($CDCl_3$, 300 MHz) δ 31.71, 103.43, 117.72,

118.17, 120.56, 121.22, 126.38, 127.07, 127.13, 127.18, 127.23, 127.67, 127.84, 127.95, 128.13, 128.36, 128.82, 129.59, 130.18, 132.14, 133.10, 133.74, 134.28, 135.29, 136.85, 138.46, 139.07, 140.26, 140.58, 141.10, 142.89, 143.89, 148.64, 151.74, 152.80, 153.97, 154.06, 154.92; MS (MALDI, positive) *m/z* = 629.2 (MH^+); HRMS (ESI^+): *m/z*: found: 629.27089, calcd for $C_{45}H_{33}N_4O_3$ (MH^+): 629.27052; UV-vis (CH_2Cl_2, λ_{max}/nm (log ε)) 448 (5.13), 609 (4.19), 766 (4.07); R_f 0.10 (CH_2Cl_2–MeOH 97 : 3).

***N*(24)-Benzyl-NCTPP (6) and *N*(22)-benzyl-NCTPP (7).** Starting from 200 mg of **1** (268 μmol) and 150 μL of benzyl bromide, **6** was obtained in 25% yield (47 mg, 67 μmol) and **7** was obtained in 9% yield (17 mg, 24 μmol).

6: ^{1}H NMR ($CDCl_3$, 300 MHz) δ −3.98 (s, 1H), −2.23 (d, *J* = 15.0 Hz, 1H), −2.11 (d, *J* = 15.0 Hz, 1H), −0.45 (br s, 1H), 5.04 (d, *J* = 7.5 Hz, 2H), 6.69 (t, *J* = 7.5 Hz, 2H), 6.82 (t, *J* = 7.5 Hz, 1H), 7.06 (d, *J* = 4.5 Hz, 1H), 7.64–7.88 (m, 15H), 8.06–8.09 (m, 1H), 8.20–8.25 (m, 3H), 8.30 (d, *J* = 4.5 Hz, 1H), 8.39 (d, *J* = 4.5 Hz, 1H), 8.43 (d, *J* = 4.8 Hz, 1H), 8.47–8.49 (m, 2H), 8.71 (d, *J* = 4.8 Hz, 1H), 8.79 (s, 1H); ^{13}C NMR ($CDCl_3$, 300 MHz) δ 47.00, 107.05, 115.58, 117.41, 120.52, 123.41, 125.00, 125.85, 127.00, 127.04, 127.23, 127.32, 127.54, 127.95, 128.82, 130.13, 131.61, 131.92, 133.54, 134.10, 135.12, 135.24, 135.33, 136.54, 138.52, 138.80, 139.62, 140.28, 141.11, 142.91, 144.01, 149.49, 150.52, 151.22, 152.73, 158.22, 159.80; MS (MALDI, positive) *m/z* = 705.2 (MH^+); HRMS (ESI^+): *m/z*: found: 705.30062, calcd for $C_{51}H_{37}N_4$ (MH^+): 705.30182; UV-vis (CH_2Cl_2, λ_{max}/nm) 448, 607, 751; R_f 0.20 (CH_2Cl_2–MeOH 97 : 3).

7: ^{1}H NMR ($CDCl_3$, 300 MHz) δ −4.71 (s, 1H), −2.91 (d, *J* = 15.0 Hz, 1H), −2.51 (d, *J* = 15.0 Hz, 1H), −0.98 (br s, 1H), 4.88 (d, *J* = 7.2 Hz, 2H), 6.64 (d, *J* = 7.2 Hz, 1H), 6.78 (d, *J* = 7.2 Hz, 1H), 7.26 (d, *J* = 4.6 Hz, 1H), 7.68–7.88 (m, 16H), 8.07–8.10 (m, 1H), 8.25 (d, *J* = 6.8 Hz, 3H), 8.30 (d, *J* = 6.8 Hz, 1H), 8.42 (d, *J* = 4.6 Hz, 1H), 8.47 (d, *J* = 4.6 Hz, 1H), 8.50 (d, *J* = 4.9 Hz, 1H), 8.76 (d, *J* = 4.9 Hz, 1H), 8.91 (s, 1H); ^{13}C NMR ($CDCl_3$, 300 MHz) δ 46.42, 103.18, 117.72, 118.74, 122.32, 122.55, 125.60, 126.20, 126.98, 127.09, 127.15, 127.23, 127.44, 127.68, 127.81, 127.88, 128.28, 128.78, 130.05, 130.28, 132.68, 133.90, 134.26, 134.52, 135.01, 135.43, 136.65, 138.24, 139.09, 139.33, 140.65, 141.19, 142.97, 143.03, 149.04, 150.94, 152.92, 153.66, 155.04, 156.57; MS (MALDI, positive) *m/z* = 705.5 (MH^+); HRMS (ESI^+): *m/z*: found: 705.30307, calcd for $C_{51}H_{37}N_4$ (MH^+): 705.30182; UV-vis (CH_2Cl_2, λ_{max}/nm) 449, 609, 766; R_f 0.13 (CH_2Cl_2–MeOH 97 : 3).

***N*(24)-Allyl-NCTPP (8) and *N*(22)-allyl-NCTPP (9).** Starting from 200 mg of **1** (268 μmol) and 150 μL of allyl bromide, **8** was obtained in 29% yield (51 mg, 78 μmol) and **9** was obtained in 15% yield (26 mg, 40 μmol).

8: ^{1}H NMR ($CDCl_3$, 300 MHz) δ −3.94 (s, 1H), −2.77 (dd, *J* = 5.5, 16.0 Hz, 1H), −2.47 (dd, *J* = 5.5, 16.0 Hz, 1H), −0.51 (br s, 1H), 3.05 (d, *J* = 16.8 Hz, 1H), 3.60 (tdd, *J* = 5.5, 10.1, 16.8 Hz, 1H), 3.97 (d, *J* = 10.1 Hz, 1H), 7.13 (d, *J* = 4.6 Hz, 1H), 7.67–7.88 (m, 14H), 8.04–8.07 (m, 1H), 8.16–8.21 (m, 4H), 8.25 (d, *J* = 4.6 Hz, 1H), 8.37 (d, *J* = 5.2 Hz, 1H), 8.42 (d, *J* = 4.9 Hz, 1H), 8.54 (d, *J* = 7.9 Hz, 2H), 8.65 (d, *J* = 5.2 Hz, 1H), 8.75 (s, 1H); ^{13}C NMR ($CDCl_3$, 300 MHz) δ 45.98, 107.48, 115.12, 115.40, 116.82, 120.30, 123.34, 124.74, 127.07, 127.18, 127.30, 127.53, 127.92, 128.09, 128.84, 130.18, 131.75, 131.82, 132.16, 133.51, 134.06, 135.05, 135.14, 136.74, 138.59, 138.87, 139.94, 140.28, 141.10, 143.02, 144.31, 149.32, 150.00, 151.27, 152.18, 158.00, 159.83; MS (MALDI, positive) *m/z* = 654.1 (M^+); HRMS (ESI^+): *m/z*: found: 655.28143, calcd for $C_{47}H_{35}N_4$ (MH^+): 655.28617; UV-vis (CH_2Cl_2, λ_{max}/nm) 448, 607, 750; R_f 0.22 (CH_2Cl_2–MeOH 97 : 3).

9: ^{1}H NMR ($CDCl_3$, 300 MHz) δ −4.77 (s, 1H), −3.41 (dd, *J* = 5.8, 15.8 Hz, 1H), −2.95 (dd, *J* = 5.8, 15.8 Hz, 1H), −1.10 (br s, 1H), 2.85 (d, *J* = 17.1 Hz, 1H), 3.42 (tdd, *J* = 5.8, 10.1, 17.1 Hz, 1H), 3.87 (d, *J* = 10.1 Hz, 1H), 7.32 (d, *J* = 4.3 Hz, 1H), 7.72–7.93 (m, 14H), 8.05–8.08 (m, 2H), 8.27 (d, *J* = 6.4 Hz, 2H), 8.38–8.43 (m, 4H), 8.46 (d, *J* = 4.9 Hz, 1H), 8.50 (d, *J* = 4.9 Hz, 1H), 8.72 (d, *J* = 5.2 Hz, 1H), 8.93 (s, 1H); ^{13}C NMR ($CDCl_3$, 300 MHz) δ 45.48, 102.49, 115.19, 117.80, 118.77, 122.17, 122.96, 126.61, 127.20, 127.25, 127.73, 128.07, 128.43, 129.10, 130.55, 131.49, 132.67, 134.21, 134.51, 135.24, 136.72, 138.40, 139.04, 140.14, 140.02, 140.98, 142.87, 150.50, 153.24, 153.45, 156.30; MS (MALDI, positive) *m/z* = 654.0 (M^+); HRMS (ESI^+): *m/z*: found: 655.28974, calcd for $C_{47}H_{35}N_4$ (MH^+): 655.28617; UV-vis (CH_2Cl_2, λ_{max}/nm) 449, 609, 769; R_f 0.10 (CH_2Cl_2–MeOH 97 : 3).

Preparation of *N*(24)-propargyl-NCTPP (10). Starting from 40 mg of **1** (54 μmol) and 200 μL propargyl bromide, **10** was obtained in 6% yield (2.0 mg, 3.0 μmol).

10: ^{1}H NMR ($CDCl_3$, 300 MHz, ppm) δ −4.12 (s, 1H), −2.82 (dd, *J* = 2.3, 17.7 Hz, 1H), −2.34 (dd, *J* = 2.3, 17.7 Hz, 1H), 1.05 (s, 1H), 7.32 (d, *J* = 4.4 Hz, 1H), 7.72–7.89 (m, 15H), 8.03 (br, 1H), 8.14–8.20 (m, 3H), 8.28 (d, *J* = 4.6 Hz, 1H), 8.38 (d, *J* = 5.1 Hz, 1H), 8.49 (d, *J* = 4.8 Hz, 1H), 8.58 (d, *J* = 7.3 Hz, 1H), 8.68 (d, *J* = 5.1 Hz, 1H), 8.77 (s, 1H); ^{13}C NMR ($CDCl_3$, 75 MHz, ppm) δ 32.88, 70.29, 106.38, 115.72, 118.39, 121.93, 123.24, 115.72, 118.39, 121.93, 123.24, 124.65, 126.92, 127.18, 127.24, 127.29, 127.35, 127.60, 127.93, 128.01, 128.13, 128.87, 130.01, 131.35, 132.34, 133.62, 134.02, 135.08, 135.57, 135.87, 136.75, 138.68, 138.93, 139.18, 140.12, 141.04, 143.04, 143.55, 149.55, 150.15, 151.56, 153.09, 158.92, 160.04; MS (MALDI, positive) *m/z* 652.7 ($[M]^+$); HRMS (ESI^+): *m/z*: found: 653.27052, calcd for $C_{47}H_{33}N_4$ (MH^+): 653.26918; UV-vis (CH_2Cl_2, λ_{max}/nm): 447, 605, 754; R_f 0.27 (CH_2Cl_2–MeOH 97 : 3).

Preparation of *N*(23)-methyl-NCTPP (13). To a solution of 5,10-diphenyl-16-methyl tripyrrane (160 mg, 0.409 mmol) and 2,4-bis(phenylhydroxymethyl)pyrrole (114 mg, 0.409 mmol) in CH_2Cl_2 (320 mL), $BF_3{\cdot}OEt_2$ (26 μL, 0.5 equiv.) was added and the reaction mixture was stirred at room temperature for 1 h under N_2. Then, DDQ (278 mg, 3 equiv.) was added and stirred for 15 min, and the crude mixture was passed through a pad of alumina. The eluent was evaporated and the residue was separated by alumina column chromatography with 0.3% MeOH in CH_2Cl_2. The green fraction was collected and concentrated to dryness to give **11** in 1% yield (2.7 mg).

13: ^{1}H NMR ($CDCl_3$, 300 MHz, ppm) δ −3.53 (s, 1H), −3.16 (s, 3H), 7.58 (d, *J* = 4.9 Hz, 1H), 7.61 (d, *J* = 4.9 Hz, 1H), 7.70–7.86 (m, 13H), 8.28–8.37 (m, 9H), 8.44 (d, *J* = 4.6 Hz, 1H), 8.50 (d, *J* = 4.6 Hz, 1H), 8.86 (s, 1H); MS (MALDI,

positive) *m/z* 629.3 ($[M]^+$); HRMS (ESI^+): *m/z*: found: 629.26920, calcd for $C_{45}H_{33}N_4$ (MH^+): 629.27052; UV-vis (CH_2Cl_2, λ_{max}/nm, (log ε)): 347 (4.33), 457 (4.89), 566 (3.86), 622 (3.89), 764 (3.85); R_f 0.38 (aluminium oxide, CH_2Cl_2–MeOH 98 : 2).

X-Ray analysis

Single crystal X-ray structural analysis for **1** was performed on a SMART APEX equipped with CCD detector (Brucker) using MoKα (graphite monochromated, λ = 0.71069 Å) radiation. X-ray analysis for **4**·CH_2Cl_2 was performed on a Saturn equipped with CCD detector (RIGAKU) using MoKα (graphite, monochromated, λ = 0.71069 Å) radiation. The data were corrected for Lorentz, polarization, and absorption effects. The structure was solved by the direct method of SHELXS-97 and refined using the SHELXL-97 program.[24] The non-hydrogen atoms were refined anisotropically by the full-matrix least-square method. The hydrogen atoms were placed at the calculated positions.

Calculation details

All density functional theory[25] calculations were achieved with a Gaussian09 program package.[26] The basis sets implemented in the program were used. The B3LYP density functional method[27] was used with a 6-31G** basis set for structural optimizations and frequency calculations and the 6-311++G** basis set was used for nucleus-independent chemical shift (NICS) calculations. Equilibrium geometries were fully optimized and verified by the frequency calculations, where no imaginary frequency was found. The NICS values were calculated with the gauge invariant atomic orbitals (GIAO) method for the optimized structures.

Acknowledgements

The present work was supported by the Grant-in-Aid for Scientific Research (21750047, 22350020, and 22655044) and the Global COE Program "Science for Future Molecular Systems" from the Ministry of Education, Culture, Sports, Science and Technology of Japan.

Notes and references

1 (*a*) T. Ding, E. A. Alemán, D. A. Modarelli and C. J. Ziegler, *J. Phys. Chem. A*, 2005, **109**, 7411; (*b*) T. Ding, J. D. Harvey and C. J. Ziegler, *J. Porphyrins Phthalocyanines*, 2005, **9**, 22.
2 (*a*) H. Furuta, T. Ishizuka, A. Osuka, H. Dejima, H. Nakagawa and Y. Ishikawa, *J. Am. Chem. Soc.*, 2001, **123**, 6207; (*b*) J. P. Belair, C. J. Ziegler, C. S. Rajesh and D. A. Modarelli, *J. Phys. Chem. A*, 2002, **106**, 6445; (*c*) J. L. Shaw, S. A. Garrison, E. A. Alemán, C. J. Ziegler and D. A. Modarelli, *J. Org. Chem.*, 2004, **69**, 7423.
3 (*a*) S. Ikeda, M. Toganoh, S. Easwaramoorthi, J. M. Lim, D. Kim and H. Furuta, *J. Org. Chem.*, 2010, **75**, 8637; (*b*) J. S. Lee, J. M. Lim, M. Toganoh, H. Furuta and D. Kim, *Chem. Commun.*, 2010, **46**, 285.
4 (*a*) H. Furuta, T. Asano and T. Ogawa, *J. Am. Chem. Soc.*, 1994, **116**, 767; (*b*) P. J. Chmielewski, L. Latos-Grażyński, K. Rachlewicz and T. Głowiak, *Angew. Chem., Int. Ed. Engl.*, 1994, **33**, 779; (*c*) T. Morimoto, S. Taniguchi, A. Osuka and H. Furuta, *Eur. J. Org. Chem.*, 2005, 3887; (*d*) M. Toganoh and H. Furuta, *Chem. Commun.*, 2012, **48**, 937.
5 (*a*) M. Toganoh and H. Furuta, *J. Phys. Chem. A*, 2009, **113**, 13953; (*b*) M. Toganoh and H. Furuta, *J. Org. Chem.*, 2010, **75**, 8213.
6 (*a*) M. Toganoh, H. Miyachi, H. Akimaru, F. Ito, T. Nagamura and H. Furuta, *Org. Biomol. Chem.*, 2009, **7**, 3027; (*b*) M. Toganoh, T. Takayama, R. Nandy, N. Kimizuka and H. Furuta, *Chem. Lett.*, 2011, **40**, 1021.
7 P. J. Chmielewski and L. Latos-Grażyński, *J. Chem. Soc., Perkin Trans. 2*, 1995, 503.
8 (*a*) W. Qu, T. Ding, A. Cetin, J. D. Harvey, M. J. Taschner and C. J. Ziegler, *J. Org. Chem.*, 2006, **71**, 811; (*b*) P. J. Chmielewski, *Org. Lett.*, 2005, **7**, 1789.
9 Z. Xiao and D. Dolphin, *Tetrahedron*, 2002, **58**, 9111.
10 (*a*) J. M. Muchowski and D. R. Solas, *J. Org. Chem.*, 1984, **49**, 203; (*b*) M. P. Edwards, A. M. Doherty, S. V. Ley and H. M. Organ, *Tetrahedron*, 1986, **42**, 3723.
11 M. Toganoh, S. Ikeda and H. Furuta, *Inorg. Chem.*, 2007, **46**, 10003.
12 (*a*) A. Srinivasan, S. K. Pushpan, M. R. Kumar, S. Mahajan, T. K. Chandrashekar, R. Roy and O. Ramamurthy, *J. Chem. Soc., Perkin Trans. 2.*, 1999, 961; (*b*) C.-H. Lee and J. L. Lindsey, *Tetrahedron*, 1994, **50**, 11427; (*c*) P. Y. Heo, K. Shin and C.-H. Lee, *Tetrahedron Lett.*, 1996, **37**, 197; (*d*) T. D. Lash, S. T. Chaney and D. T. Richter, *J. Org. Chem.*, 1998, **63**, 9076.
13 All the experimental data were remeasured for this manuscript. Theoretical data are taken from ref 5.
14 Small amounts of the type-A isomer (less than 10%) was detected by ^{1}H NMR in DMF-d_7 at ambient temperature.
15 (*a*) P. v. R. Schleyer, C. Maerker, A. Dransfeld, H. Jiao and N. v. E. Hommes, *J. Am. Chem. Soc.*, 1996, **118**, 6317; (*b*) Z. Chen, C. S. Wannere, C. Corminboeuf, R. Puchta and P. v. R. Schleyer, *Chem. Rev.*, 2005, **105**, 3842.
16 (*a*) T. M. Krygowski and M. Cyrański, *Tetrahedron*, 1996, **52**, 10255; (*b*) T. M. Krygowski and M. Cyrański, *Chem. Rev.*, 2001, **101**, 1385.
17 No solvent effect was taken into consideration in TDDFT calculations and thus the theoretical wavelengths tend to be shorter than the experimental wavelengths.
18 (*a*) H. Furuta, T. Ishizuka, A. Osuka and T. Ogawa, *J. Am. Chem. Soc.*, 1999, **121**, 2945; (*b*) H. Furuta, T. Ishizuka, A. Osuka and T. Ogawa, *J. Am. Chem. Soc.*, 2000, **122**, 5748; (*c*) T. Ishizuka, S. Ikeda, M. Toganoh, I. Yoshida, Y. Ishikawa, A. Osuka and H. Furuta, *Tetrahedron*, 2008, **64**, 4037.
19 M. Toganoh, T. Kimura and H. Furuta, *Angew. Chem., Int. Ed.*, 2008, **47**, 8913.
20 M. Toganoh, T. Hihara and H. Furuta, *Inorg. Chem.*, 2010, **49**, 8182.
21 (*a*) M. Toganoh, T. Kimura and H. Furuta, *Chem. Commun.*, 2008, 102; (*b*) M. Toganoh, T. Kimura and H. Furuta, *Chem.–Eur. J.*, 2008, **14**, 10585.
22 N. Kashiwagi, T. Akeda, T. Morimoto, T. Ishizuka and H. Furuta, *Org. Lett.*, 2007, **9**, 1733.
23 N. Grzegorzek, M. Pawlicki and L. Latos-Grażyński, *J. Org. Chem.*, 2009, **74**, 8547.
24 G. M. Sheldrick, *Program for the Solution of Crystal Structures*, University of Göttingen, Göttingen, Germany, 1997.
25 (*a*) P. Hohenberg and W. Kohn, *Phys. Rev.*, 1964, **136**, B864; (*b*) W. Kohn and L. Sham, *J. Phys. Rev.*, 1965, **140**, A1133.
26 M. J. Frisch, G. W. Trucks, H. B. Schlegel, G. E. Scuseria, M. A. Robb, J. R. Cheeseman, G. Scalmani, V. Barone, B. Mennucci, G. A. Petersson, H. Nakatsuji, M. Caricato, X. Li, H. P. Hratchian, A. F. Izmaylov, J. Bloino, G. Zheng, J. L. Sonnenberg, M. Hada, M. Ehara, K. Toyota, R. Fukuda, J. Hasegawa, M. Ishida, T. Nakajima, Y. Honda, O. Kitao, H. Nakai, T. Vreven, J. A. Montgomery, Jr., J. E. Peralta, F. Ogliaro, M. Bearpark, J. J. Heyd, E. Brothers, K. N. Kudin, V. N. Staroverov, T. Keith, R. Kobayashi, J. Normand, K. Raghavachari, A. Rendell, J. C. Burant, S. S. Iyengar, J. Tomasi, M. Cossi, N. Rega, J. M. Millam, M. Klene, J. E. Knox, J. B. Cross, V. Bakken, C. Adamo, J. Jaramillo, R. Gomperts, R. E. Stratmann, O. Yazyev, A. J. Austin, R. Cammi, C. Pomelli, J. W. Ochterski, R. L. Martin, K. Morokuma, V. G. Zakrzewski, G. A. Voth, P. Salvador, J. J. Dannenberg, S. Dapprich, A. D. Daniels, O. Farkas, J. B. Foresman, J. V. Ortiz, J. Cioslowski and D. J. Fox, *GAUSSIAN 09, Revision B.01*, Gaussian, Inc., Wallingford CT, 2010.
27 (*a*) A. D. Becke, *J. Phys. Chem.*, 1993, **98**, 5648; (*b*) C. Lee, W. Yang and R. G. Parr, *Phys. Rev. B*, 1988, **37**, 785; (*c*) S. H. Vosko, L. Wilk and M. Nusair, *Can. J. Phys.*, 1980, **58**, 1200; (*d*) P. J. Stephens, F. J. Devlin, C. F. Chabalowski and M. J. Frisch, *J. Phys. Chem.*, 1994, **98**, 11623.